Journal of Agricultural Science; Vol. 15, No. 9; 2023
ISSN 1916-9752 E-ISSN 1916-9760
Published by Canadian Center of Science and Education

Analyzing the Characteristics of Cropping Intensity's Change of Cultivated Land in China During 2010-2019

Yuanhong You[1,2], Yuhao Zhang[1], Haiyan Hou[3,4] & Zhiguang Tang[4]

[1] School of Geography and Tourism, Anhui Normal University, Wuhu, China

[2] Engineering Technology Research Center of Resource Environment and GIS, Wuhu, China

[3] School of Earth Sciences and Spatial Information Engineering, Hunan University of Science and Technology, Xiangtan, China

[4] National-Local Joint Engineering Laboratory of Geo-Spatial Information Technology, Hunan University of Science and Technology, Xiangtan, China

Correspondence: Yuanhong You, School of Geography and Tourism, Anhui Normal University, Wuhu 241002, China. Tel: 1-889-382-0872. E-mail: youyh@ahnu.edu.cn

Received: June 18, 2023 Accepted: July 19, 2023 Online Published: August 15, 2023

doi:10.5539/jas.v15n9p10 URL: https://doi.org/10.5539/jas.v15n9p10

Abstract

The sustained stability of the arable land replanting index is crucial to the national food security strategy. The exploration of the temporal and spatial changes in the arable land replanting index is of great significance for agricultural development and food security evaluation. This study investigates China's arable land replanting index from 2010 to 2019 using MODIS NDVI image data, S-G filtering, and quadratic differentiation methods. The results show that there are significant spatial differences in China's arable land replanting index, with the Huang-Huai-Hai region mainly producing double-cropping crops, the Northeast Plain and Loess Plateau mainly producing single-cropping crops, and the area south of the Yangtze River mainly producing multiple-cropping crops. Overall, China's food production is mainly based on single-season crops. There is a gradual shift towards double-season crops from north to south, with lower replanting indices in the northwest and higher indices in the eastern provinces. The south has significantly higher indices than the north. During the study period, the arable land replanting index showed an overall upward trend. There were significant increases in the replanting index in the northeast, the Loess Plateau, and the northern Huang-Huai-Hai region. However, there was a downward trend in the southern Huang-Huai-Hai region and the middle and lower reaches of the Yangtze River. It is crucial to maintain the effective planting area of arable land in the Loess Plateau and the double-season planting area of arable land in the Huang-Huai-Hai region while also addressing the downward trend of the arable land replanting index in the middle and lower reaches of the Yangtze River to ensure food security by stabilizing the index.

Keywords: replanting index, food security, arable land, NDVI time series

1. Introduction

Farmland is the basic resource for food production and a necessary condition for human survival (Ray et al., 2012). With the development of China's urbanization process and population growth, the area of cultivated land is gradually decreasing, and the conflict between people and land is becoming increasingly acute, which has become the main factor affecting China's food security (Foley et al., 2005). As a populous country, China has a huge demand for food. Fully utilizing farmland resources to increase food production can promote national production and economic development. The number of times a piece of farmland is cultivated during a specific period can directly affect the output of food. The cropping index is an important indicator reflecting the average number of crops planted on farmland in a year (Godfray et al., 2010; Yan et al., 2014). On the one hand, the cropping index can reflect the degree of farmland cropping; on the other hand, it is a basic parameter used to evaluate the use of farmland resources at the regional scale. According to data from the Food and Agriculture Organization of the United Nations in 2017, China's total amount of cultivated land accounts for 9% of the world's total, and the per capita arable land area is only 45% of the global average. In addition, due to the significant differences in geographical characteristics between North and South China, farmland is unevenly distributed in geographic space, resulting in significant differences in food ripening in different regions.

Compared with cultivating new land, increasing the number of crop plantings on existing farmland can maximize the utilization of farmland resources and increase food production. Improving the cropping index has become an important way to promote grain production and is an important measure to ensure food security (Foley et al., 2011; Ray & Foley, 2013; Estel et al., 2016). Therefore, exploring the spatiotemporal changes of the cropping index can provide a scientific basis for agricultural production, farmland utilization, and land use planning, and at the same time, it is of great significance to ensure national food security.

With the rapid development of remote sensing technology, a large number of studies have shown that remote sensing data inversion-related indices can well reflect the vegetation growth status, and long-time series remote sensing data is an important way to obtain the cropping index (Kuenzer & Knauer, 2013; Satyawan & Hooda, 2014; Marshall & Thenkabail, 2015; Cian et al., 2018). Large-scale crop mapping is considered one of the most important applications of satellite-based remote sensing (Jiang et al., 2020; Ibrahim et al., 2021). Earlier, crop coverage mapping was done by several researchers using Landsat, Satellite Pourl'Observation de la Terre (SPOT), Moderate Resolution Imaging Spectroradiometer (MODIS), Sentinel-2 (Friedl et al., 2002; Butt et al., 2015; Mishra et al., 2019; Yang et al., 2019). Among the other satellites, Sentinel-2 (constellation of two satellites, viz. Sentinel-2A, and 2B), equipped with the Multispectral Instrument (MSI) and offering 5-day interval image in thirteen spectral bands ranging from visible and near-infra-red (NIR) to short-wave infrared (SWIR) at 10 m, 20 m, and 60 m spatial resolutions, is one of the most applicable earth observation satellites for land-use study. The satellite covers a swath of 290 km (Ramoelo et al., 2015; Veloso et al., 2017). Although the cropping intensity and the per capita cropped land holding in the Indian Sundarbans region were estimated earlier, the yearly variation of the cropping intensity and the seasonality of cropped land per capita/households have not been investigated yet. To bridge the gap, the present study was conducted in the Gosaba Community Development block of Indian Sundarbans to assess the spatiotemporal dynamics of cropping intensities in the 2017-2018, 2018-2019, and 2019-2020 cropping years. Seasonal variability of the cropped land per household was estimated. Multi-temporal Sentinel-2 data were used for cropping sequence and cropping intensity mapping using. The seasonal crop-fallow maps were reclassified under the rule-based classification approach for the three cropping years. The influence of the winter and summer season surface water availability and rainfall pattern on the cropping intensity was investigated in the present study.

In this study, we attempted to assess the spatiotemporal changes in cropping intensity in China from 2010-2019 using a rule-based algorithm on time series MODIS normalized difference vegetation index (NDVI). The results from this study can provide informational support for making cropland use policy, which is important for food security in China.

2. Data and Method

2.1 Data Source

2.1.1 MODIS NDVI

Compared with other remote sensing data, there are several reasons why MODIS data can be widely used. Firstly, it is because of its simple acquisition method. Secondly, it has a wide spectral range with 36 bands and small intervals between different bands, which can better image ground objects and reflect more detailed features of land cover, allowing for a more complete calculation of NDVI values for vegetation growth. Additionally, MODIS data has a high update frequency, which is of great value for real-time regional observations.

This study uses the MODIS Level 3 composite product MODIS13A2, which is available on the United States Geological Survey (USGS) website. The spatial resolution of this data is 1 km, with a temporal resolution of 16 days, and there are a total of 23 image data sets per year. The biggest advantage of this dataset is that it has been pre-processed for aerosols, mixed clouds, and snow cover, and is already in the form of NDVI data products. Therefore, there is no need for manual calibration or additional calculations, and the data has strong continuity with almost no missing values during the research period selected in this study.

2.1.2 Cropland Data

In this study, we selected the cropland data from China's National Land-Use/Cover Change Dataset (NLCD-China) at a mapping scale of 1: 100000 by the Chinese Academy of Sciences. The NLCD-China dataset was produced using visual interpretation of the 30 m Landsat TM/ETM images (Liu et al., 2014; Yan et al., 2018). The cropland dataset used in this paper was extracted from the NLCD-China dataset which was assumed to have high accuracy. We extracted China's cultivated land data for 2015, as shown in Figure 1. From the figure, it can be seen that China's cultivated land is mainly distributed in the coastal eastern monsoon region, and there are significant differences in its distribution between the north and south. If we take the Qinling

Mountains-Huaihe River line as a reference for the division of northern and southern climates in China, the area south of this line is mainly a rice paddy distribution zone, while the area north of this line is mainly dominated by dryland farming.

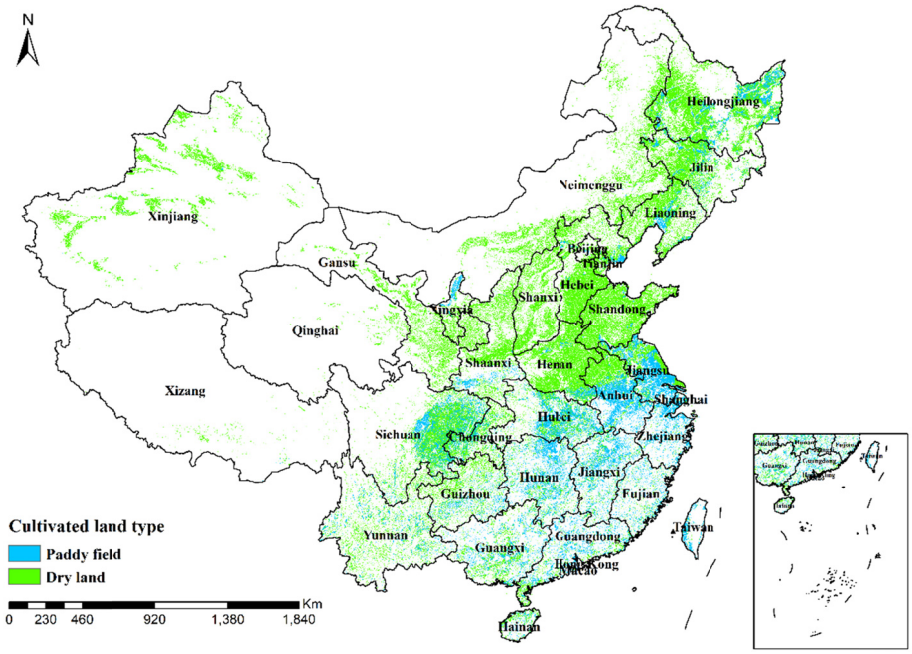

Figure 1. Distribution map of cultivated land utilization in China in 2015

2.2 Methods

2.2.1 The Relationship Between the Replanting Index and NDVI Time Series

In the study of the replanting index, normalized difference vegetation index (NDVI) data is required, with values ranging between -1 and 1. When the land cover type is snow or water, the NDVI value is less than 0; when the land cover type is rock or bare soil, the NDVI value is equal to 0; when the land cover type is vegetation, the NDVI value is greater than 0 and increases with the increase of vegetation coverage. Therefore, NDVI data can be used to monitor the growth status of vegetation and the proportion of surface vegetation coverage and is currently widely used to monitor the phenological status of various crops.

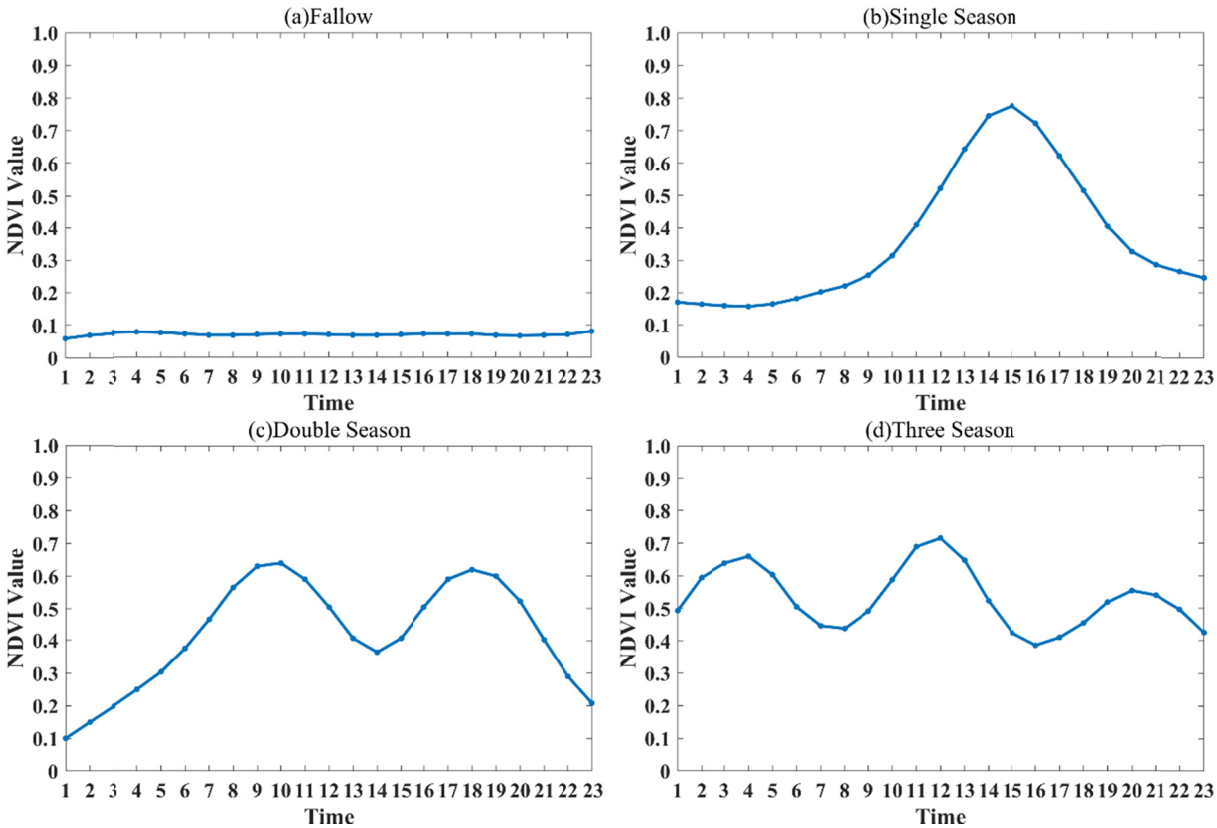

Figure 2. The time series NDVI curves of different cooked crops in 2011

Time series analysis is a method of continuous remote sensing monitoring over a specific area for a long period of time, extracting features from remote sensing images to analyze the regularity of changes in time series curves (Estel et al., 2016). The MODIS NDVI product has a total of 23 images per year, and for a single pixel on an image, there are 23 different NDVI values corresponding to different periods, which can reflect the growth status of vegetation at different times. At the same time, the change cycle of the curve can accurately reflect a complete growth cycle of crops from germination to withering. Typically, during the planting and harvesting of crops, the NDVI value is low, corresponding to the trough position of a continuous curve; when the crops are in their most vigorous growth stage, the NDVI value is high, corresponding to the peak position of a continuous NDVI curve. A single peak in the time series curve indicates that the region is a one-crop-per-year area (as shown in Figure 2b), two peaks indicate a two-crop-per-year area (as shown in Figure 2c), and three peaks indicate a three-crop-per-year area (as shown in Figure 2d). The NDVI values of fallow land are relatively low, and the time series curve is generally flat with little variation within a year (as shown in Figure 2a). Therefore, the extraction of a replanting index can be considered as the extraction of peak frequency.

2.2.2 Savitzky-Golay Filtering Reconstruction of NDVI Time Series

Considering that vegetation indices directly obtained from remote sensing images have a lot of noise and cannot be used directly to construct NDVI time series curves, it is necessary to perform denoising processing on the original data. Currently, there are many methods for removing noise, with the most commonly used being Savitzky-Golay (SG) filtering, double logistic function filtering (D-L), asymmetric Gaussian filtering (A-G), and Fourier harmonic (HANTS harmonic) filtering. The biggest advantage of S-G filtering is that it can smooth the filter while maximizing the retention of the change information in remote sensing images, thus providing a clearer description of the detailed changes in time series data. Therefore, we chose S-G filtering to reconstruct the NDVI time series curve. S-G filtering was proposed by Savitzky and Golay and is a filtering method based on local polynomial least squares fitting in the time domain. By selecting a certain number of neighboring values near a point and using the least squares method to fit an n-th order polynomial, the smoothing value of that point can be calculated using the fitted polynomial. This method can describe the small dynamic changes of NDVI during the year in China's mainland under various cropping systems and can preserve high-order moments by finding a suitable filtering coefficient. The calculation formula is as follows:

$$Y_j^* = \frac{\sum_{i=-m}^{m} C_i \times Y_{j+i}}{N} \tag{1}$$

In the equation, Y_i^* is the NDVI fitting value, Y_{j+i} is the original NDVI value, C_i is the filtering coefficient of the ith NDVI value, N is the size of the sliding window, which also represents the number of convolutions, and the smoothing array contains $2m + 1$ points, where m is half of the smoothing window size. Considering the edge effect of S-G filtering, the first few data points and the last few data points of each year cannot be well processed. Therefore, when reconstructing the NDVI time series curve for each year, the last n temporal data from the previous year and the first n temporal data from the following year are combined with the NDVI sequence of that year to ensure the smoothness of NDVI at each temporal point of every year and guarantee the reliability of the data. After the S-G filtering smoothing process, not only the noise impact on the NDVI time series curve is removed, but the accuracy of subsequent results is also improved, which can accurately reflect the growth status of vegetation. Figure 3 shows a comparison of the NDVI time series curve of the pixel before and after S-G filtering, with the horizontal axis representing the period of remote sensing images and the vertical axis representing the NDVI value.

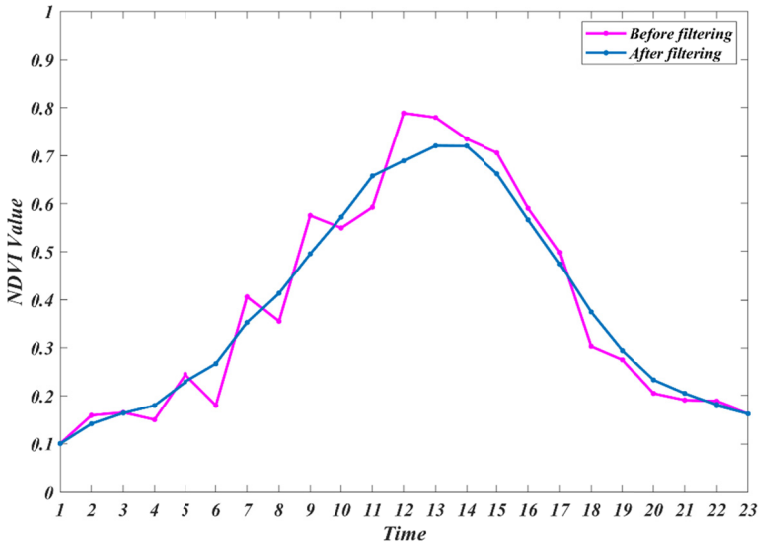

Figure 3. Comparison of timing NDVI curves before and after S-G filter denoising and smoothing

2.2.3 Second Difference Method

There are two main methods for obtaining the replanting index of arable land: direct comparison and second difference. The direct comparison method compares the vegetation index value of each time point with the adjacent vegetation index values before and after it to obtain the peak value within that interval and then counts the number of peaks in one year. The second difference method is similar to the peak value method. It arranges the N NDVI values of a single pixel in one year in chronological order as an array and then obtains the frequency of peaks of the single pixel in one year. Compared with the direct comparison method, the second difference method has higher accuracy. In this study, the number of peak frequencies and the time points at which they are reached in the NDVI time series curve were extracted using the second difference method based on pixel-level analysis and used as the judging index for the replanting index. The specific calculation method of the second difference method is as follows:

First, use Formula 2 to calculate the adjacent NDVI differences and obtain the S_1 sequence. Then, use Formula 3 to determine the positive and negative values of the S_1 sequence and reassign them. If it is a negative value, it is recorded as -1; if it is a positive value, it is recorded as 1, resulting in the S_2 sequence. Finally, according to Formula 4, calculate the difference between the front and back sequences of S_2, and record it as S_3. The formulas are as follows:

$$S_{1i} = V_{NDVI_i} - V_{NDVI_i - 1} \tag{2}$$

$$S_{2i} = \begin{cases} -1, S_{1i} < 0 \\ 1, S_{1i} > 0 \end{cases} \tag{3}$$

$$S_{3i} = S_{2i+1} - S_{2i} \tag{4}$$

where, i represents the ith element in the sequence. At this point, there are $n - 1$ elements in the sequence, and calculating the difference between the front and back elements of the sequence yields a sequence consisting of -2, 0, and 2, with $n - 2$ elements. It can be determined that the peak of the sequence will appear at the position where the element in the S_3 sequence is -2 and both the front and back elements are 0. The second difference method is very sensitive to peaks, and although the time series curve has been smoothed, false peaks may still appear in practice, leading to decreased accuracy. Therefore, the following issues need to be considered in practical situations: 1) the NDVI time series curve of bare land is not completely flat and may have fluctuating "peaks". 2) small peaks may occur outside the crop growing season and need to be eliminated by setting relevant restrictions based on the actual growth of crops. Considering that most bare land NDVI values are low, we set the NDVI value of the peak to be greater than 0.4 to eliminate the influence of bare land peaks. In addition, considering that the maturity time of most crops in most areas is more than three months, we set the interval between two peak values in the NDVI time series curve to be more than three months based on the characteristics of crop growth cycles to reduce errors caused by small peaks.

2.2.4 The Calculation Method of the Replanting Index

The average replanting index in the study area can be calculated according to the definition of the replanting index using the following equation:

$$C_1 = \sum_{i}^{n} \frac{M_i}{N} \times 100\% \tag{5}$$

where, M represents the peak frequency of the ith year pixel in the study area, N represents the number of arable land pixels in the region, and C_1 represents the average replanting index of arable land.

3. Results and Discussion

3.1 Spatial Distribution of the National Replanting Index

Figure 4 shows the spatial distribution of the replanting index of arable land from 2010 to 2019. The value "0" in the legend represents pixels with a peak count of zero in the sequence, indicating that these areas are fallow land. The value "1" represents pixels with a peak count of one in the sequence, which means that single-season crops are planted in this area. The value "2" represents pixels with a peak count of two in the sequence, indicating that double-season crops are planted in this area. The value "3" represents pixels with a peak count of three in the sequence, indicating that triple-season crops are planted in this area. To facilitate analysis, we divided China's arable land into nine agricultural regions according to the agricultural zoning map, namely the Northeast Plain region, the Huang-Huai-Hai Plain region, the Loess Plateau region, the Yangtze River Middle and Lower Reaches region, the South China region, the Yunnan-Guizhou Plateau region, the Sichuan basin region, the Qinghai-Tibet Plateau region, and the northern semi-arid region. From Figure 4, it can be seen that there are significant spatial differences in the replanting index of arable land on the mainland of China. The northern regions, including the Northeast Plain and the Loess Plateau, are mainly dominated by single-season crops, while the Huang-Huai-Hai region, the Yangtze River Middle and Lower Reaches region, the southwestern region, and the South China region are mainly a combination of single and double-season crops, with some areas having a small number of triple-season crops.

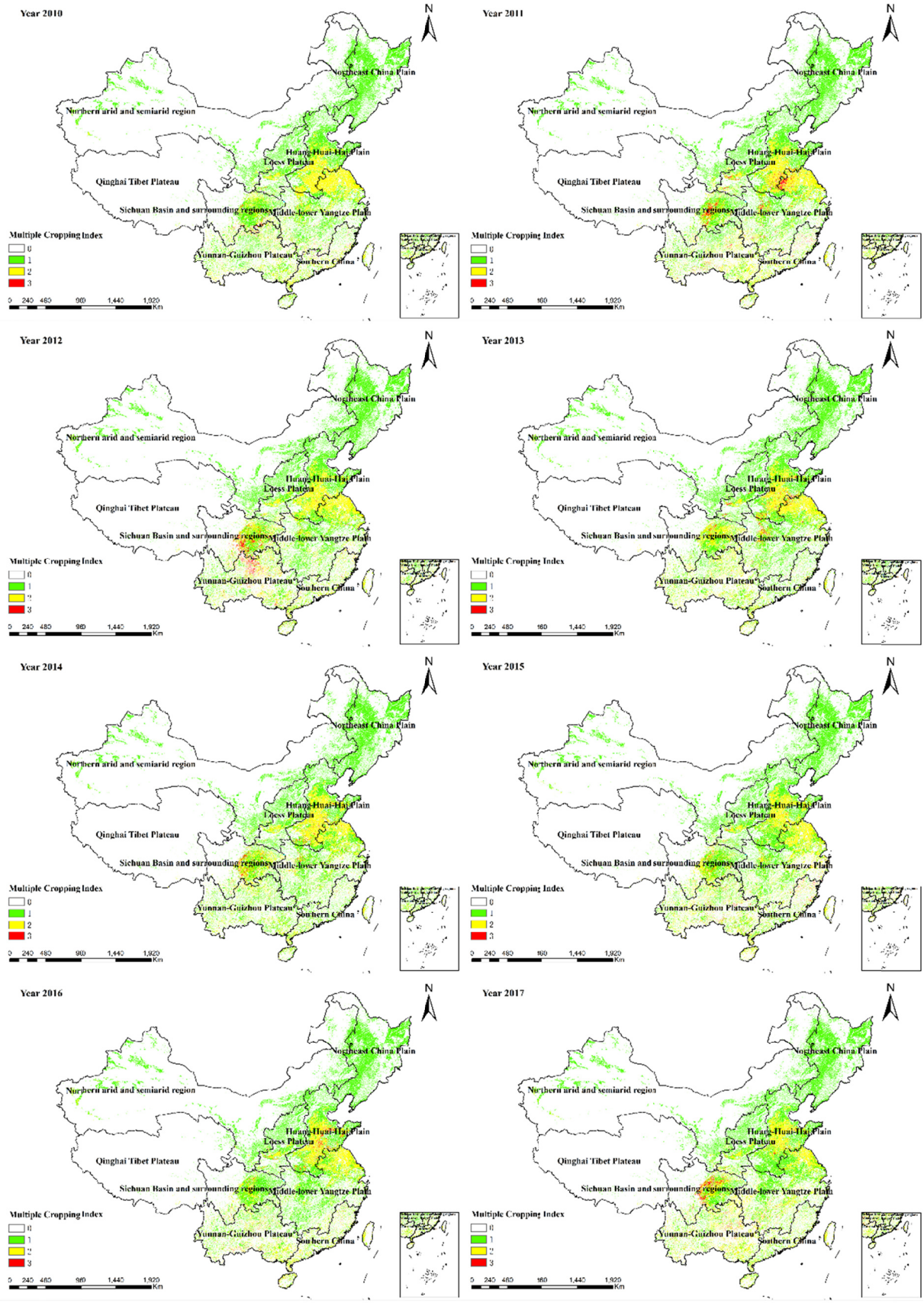
Year 2010
Year 2011
Year 2012
Year 2013
Year 2014
Year 2015
Year 2016
Year 2017
N
Northeast China Plain
Northern arid and semiarid region
Huang-Huai-Hai Plain
Loess Plateau
Qinghai Tibet Plateau
Sichuan Basin and surrounding regions
Middle-lower Yangtze Plain
Yunnan-Guizhou Plateau
Southern China
Multiple Cropping Index
0
1
2
3
0 240 480 960 1,440 1,920
Km

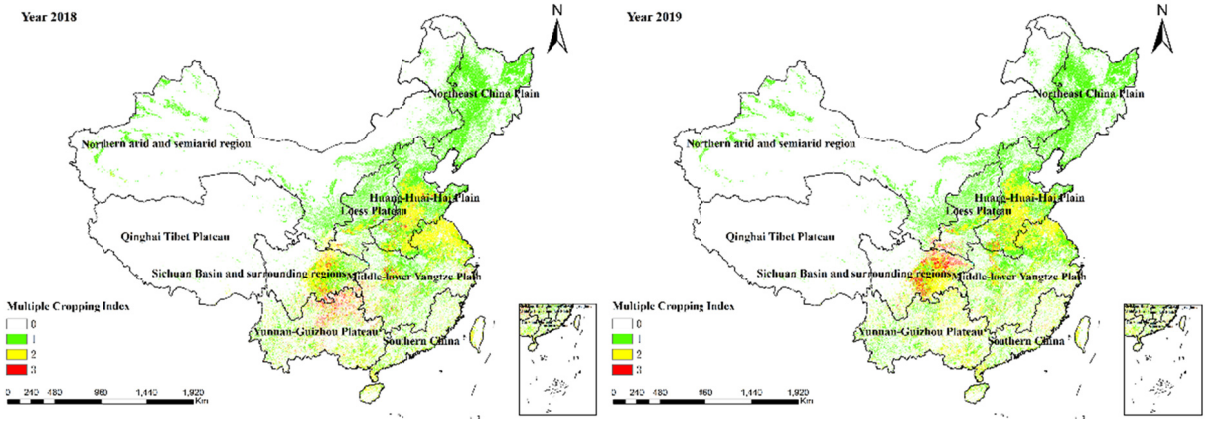

Figure 4. Spatial distribution map of China's cultivated land multiple cropping index from 2010 to 2019

Overall, the replanting index of arable land in China gradually increases from single-season to double-season from north to south. The main reason for this spatial difference is that crop growth is affected by climate factors. The climate in northern China is dry, with a lower average annual temperature and some areas experiencing seasonal frost, making it unsuitable for crop growth and further limiting the replanting index of arable land in these areas. In contrast, the Huang-Huai-Hai region, the Yangtze River Middle and Lower Reaches region, the southwestern region, and the South China region have a humid climate, with adequate rainfall throughout the year and a higher average annual temperature, which is conducive to crop growth. Therefore, the replanting index of arable land in these areas is higher. Qinghai and Tibet are located in high-altitude regions with few arable lands, and only a small number of single and double-season crops are distributed in their southeastern parts. Further analysis showed that single-season crops accounted for approximately 68% of the total arable land area in China, double-season crops accounted for approximately 23% of the total arable land area, and triple-season crops accounted for approximately 1% of the total arable land area. This is essentially close to the research findings of Xie and Liu, 2015. Hence, it can be concluded that single-season crops are mainly grown on arable land in mainland China, with a small number of areas having triple-season crops.

3.2 Analysis of the Evolution of the National Replanting Index

To further explore the changes in the replanting index of arable land during the study period, we compared the replanting index of arable land in 2019 and 2010. By taking the difference between the replanting indices of corresponding pixels in these two years, we analyzed the changes in the national replanting index of arable land over the past decade. Figure 5 shows the difference in the replanting index of arable land between 2010 and 2019.

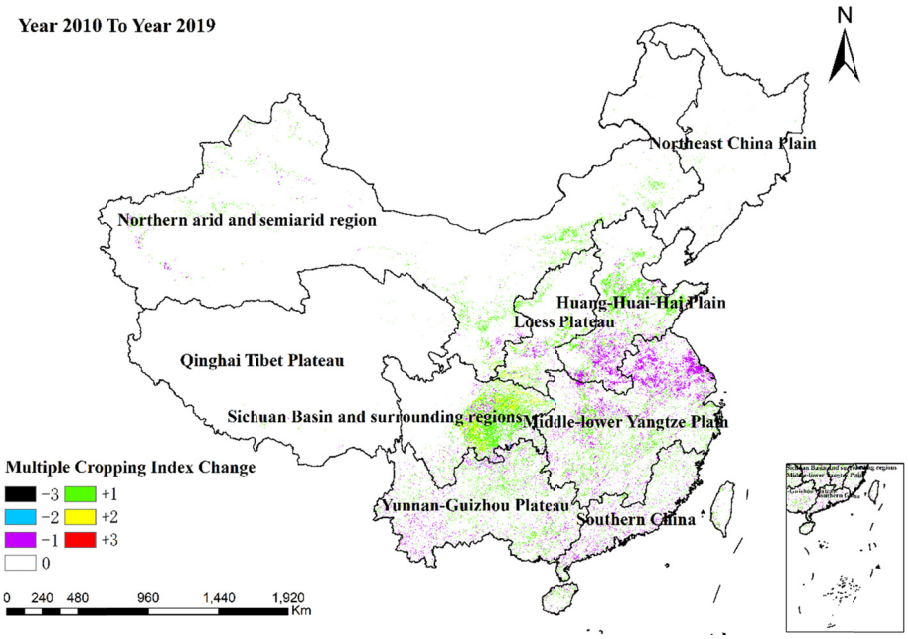

Figure 5. Distribution map of changes in China's cultivated land multiple cropping index from 2010 to 2019

From Figure 5, it can be seen that the replanting index of most areas in the country is on the rise. The replanting index of the Northeast Plain region, the Huang-Huai-Hai Plain region, and the Loess Plateau region are mainly on the rise, while the replanting index of the Yangtze River Middle and Lower Reaches region is mainly on the decline. Further statistical analysis revealed that the area where the replanting index is on the rise is approximately twice as large as the area where the replanting index is on the decline. Figure 6 shows the annual average replanting index from 2010 to 2019, which indicates that the national average replanting index has been on an upward trend over the past ten years, with a replanting index greater than 1.1 each year. This indicates that replanting has been implemented on arable land in most regions of China. In addition, Figure 6 shows that the average replanting index in 2019 was the highest, reaching 1.2. Furthermore, we conducted a statistical analysis of the proportion of crops grown in different seasons in China from 2010 to 2019. Figure 7 shows the proportion and trend of crops grown in different seasons. From the figure, it can be seen that the proportion of fallow land is gradually decreasing during the study period, while the proportion of single and double-season crops is increasing, but the change in the proportion of triple-season crops is not significant. The above research results indicate that the reason why the national replanting index of arable land has been continuously increasing during the study period is due to the gradual transformation of fallow land into crop planting, an increase in the number of areas switching from single-season to double-season crops, and more areas with changed crop types or fallow land being used for crop planting compared to areas with no change or a switch from crops to fallow land.

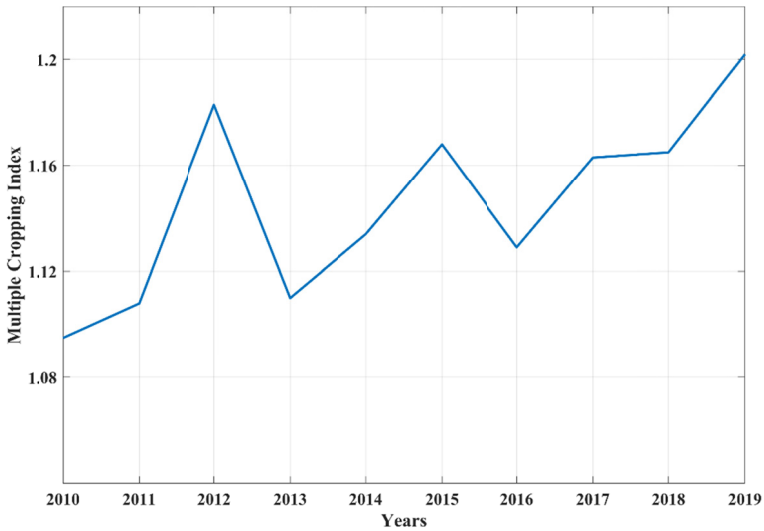

Figure 6. Changes in the average multiple cropping index from 2010 to 2019

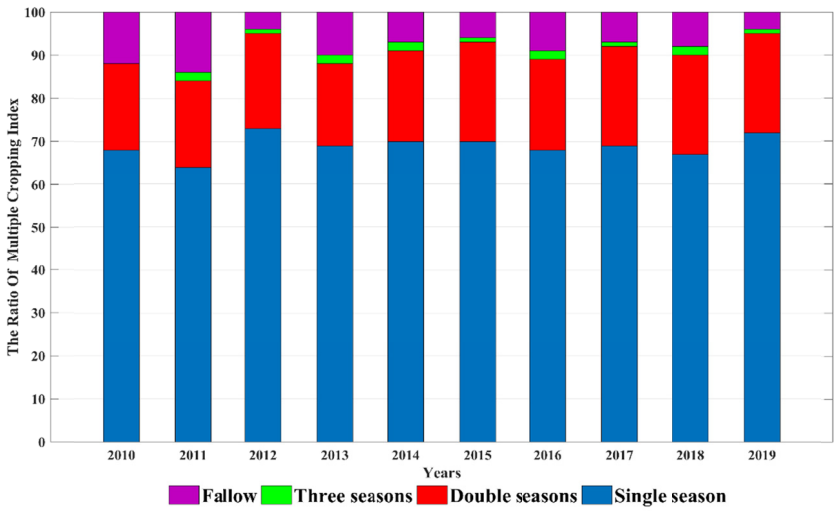

Figure 7. The proportion and change trend of crops in different seasons in the country year by year

3.3 Analysis of Significant Changes in the Replanting Index Region

From Figure 4, it can be seen that the replanting index of the Northeast Plain region, the Huang-Huai-Hai Plain region, the southwestern region, the Loess Plateau region, and the Yangtze River Middle and Lower Reaches region has undergone significant changes during the study period. Therefore, we extracted the replanting index of arable land in these regions separately for further discussion.

From Figure 8, it can be seen that the Northeast Plain region is mainly dominated by the planting of single-season crops, with a range of the regional average replanting index between 0.6 and 1.0, and the spatial distribution of the replanting index shows a trend of being higher in the south and lower in the north. It can be seen from Figure 8 that the replanting index of the Northeast Plain region has been on the rise from 2010 to 2019, mainly due to the gradual reduction of fallow land in this area and the continuous increase in the proportion of single-season crop planting. Regarding the spatial distribution of the replanting index in the Northeast Plain region, a considerable portion of the fallow land has been converted to planting single-season crops, mainly distributed in the eastern and northwestern parts of the region.

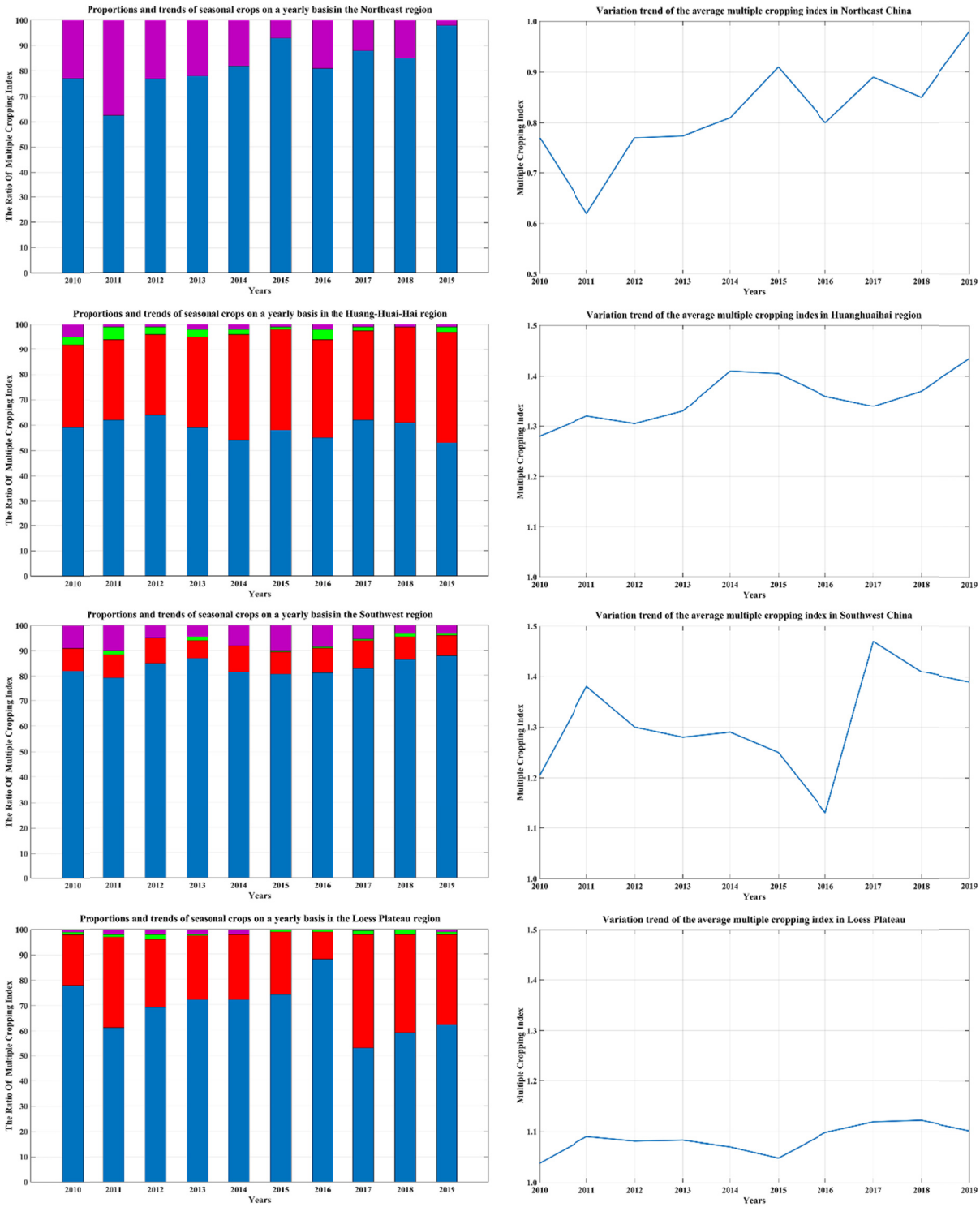
Proportions and trends of seasonal crops on a yearly basis in the Northeast region
The Ratio Of Multiple Cropping Index
Years
Variation trend of the average multiple cropping index in Northeast China
Multiple Cropping Index
Years
Proportions and trends of seasonal crops on a yearly basis in the Huang-Huai-Hai region
The Ratio Of Multiple Cropping Index
Years
Variation trend of the average multiple cropping index in Huanghuaihai region
Multiple Cropping Index
Years
Proportions and trends of seasonal crops on a yearly basis in the Southwest region
The Ratio Of Multiple Cropping Index
Years
Variation trend of the average multiple cropping index in Southwest China
Multiple Cropping Index
Years
Proportions and trends of seasonal crops on a yearly basis in the Loess Plateau region
The Ratio Of Multiple Cropping Index
Years
Variation trend of the average multiple cropping index in Loess Plateau
Multiple Cropping Index
Years

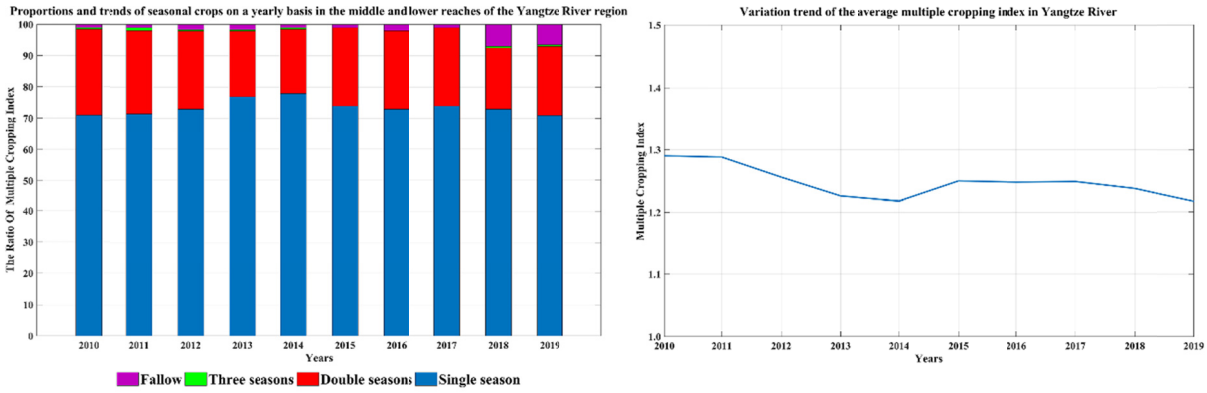

Figure 8. The annual proportion and change trend of crops in different seasons and Variation trend of the average multiple cropping index in Northeast China and Huang-Huai-Hai region and Southwest China and Loess Plateau and Yangtze River

Compared to the Northeast Plain region, the replanting index in the Huang-Huai-Hai region is slightly higher, with a range of the regional average replanting index between 1.25 and 1.45 and the spatial distribution of the replanting index showing a pattern of being higher in the south and lower in the north. Considering the changes in the replanting index of the Huang-Huai-Hai region over the past decade, there are differentiated spatial changes in the replanting index in this area. In the northern part of the Huang-Huai-Hai region, such as Shandong Province, a large area of single-season crop planting has been converted into double-season crop planting, resulting in an upward trend in the replanting index, which is related to the continuous increase in the planting area of corn. However, in the southern part of the Huang-Huai-Hai region, a large area of double-season crop planting has been converted into single-season crop planting, leading to a decrease in the replanting index in this area. Although the replanting index in the Huang-Huai-Hai region has been on an overall upward trend, there were two periods, i.e., 2011-2012 and 2014-2017, during which the replanting index in this area showed a downward trend.

The southwestern region is dominated by mixed single and double-season crop planting but with more single-season crops, resulting in a higher average replanting index, ranging from 1.2 to 1.5. From Figure 9, it can be seen that the spatial distribution of the replanting index shows a pattern of being higher in the east and lower in the west, mainly since the eastern part of this region is mainly plain areas with better soil productivity, suitable for crop rotation. The northwestern part of this region is mainly composed of high-altitude areas, with seasonally frozen soil and poorer soil productivity, leading to weaker crop rotation capabilities in the northwest. It can be seen from Figure 8 that the replanting index of arable land in the southwestern region has mainly been on an upward trend from 2011 to 2019, mainly due to the continuous increase in the proportion of double-season crop planting in this region. As Figure 9 shows that the areas where single-season crop planting was changed to double-season crop planting are mainly concentrated in the central and southern parts of this region, indicating that these areas have great potential for crop planting on arable land.

The Loess Plateau region is mainly dominated by single-season crop planting, with a small amount of double-season crops, and the average replanting index of the entire region is in the range of 1.04-1.12, at a relatively low level. The spatial distribution of the replanting index shows a pattern of being higher in the west and lower in the east, mainly due to the dual influence of climate and terrain in this region. The terrain in this region is higher in the west and lower in the east, and the climate in the central and southern parts is warm and humid, suitable for crop growth, while the climate in the northwest is dry and unfavorable for crop growth. From Figure 8, it can be seen that the replanting index in the Loess Plateau region has been on an overall upward trend, and the increase in the replanting index has accelerated since 2015, with the proportion of fallow land continuously decreasing. This is mainly due to the conversion of a considerable portion of fallow land into single-season crop planting in this region. In addition, the implementation of ecological projects such as the "Three-North" project in this region has greatly improved the local ecological environment.

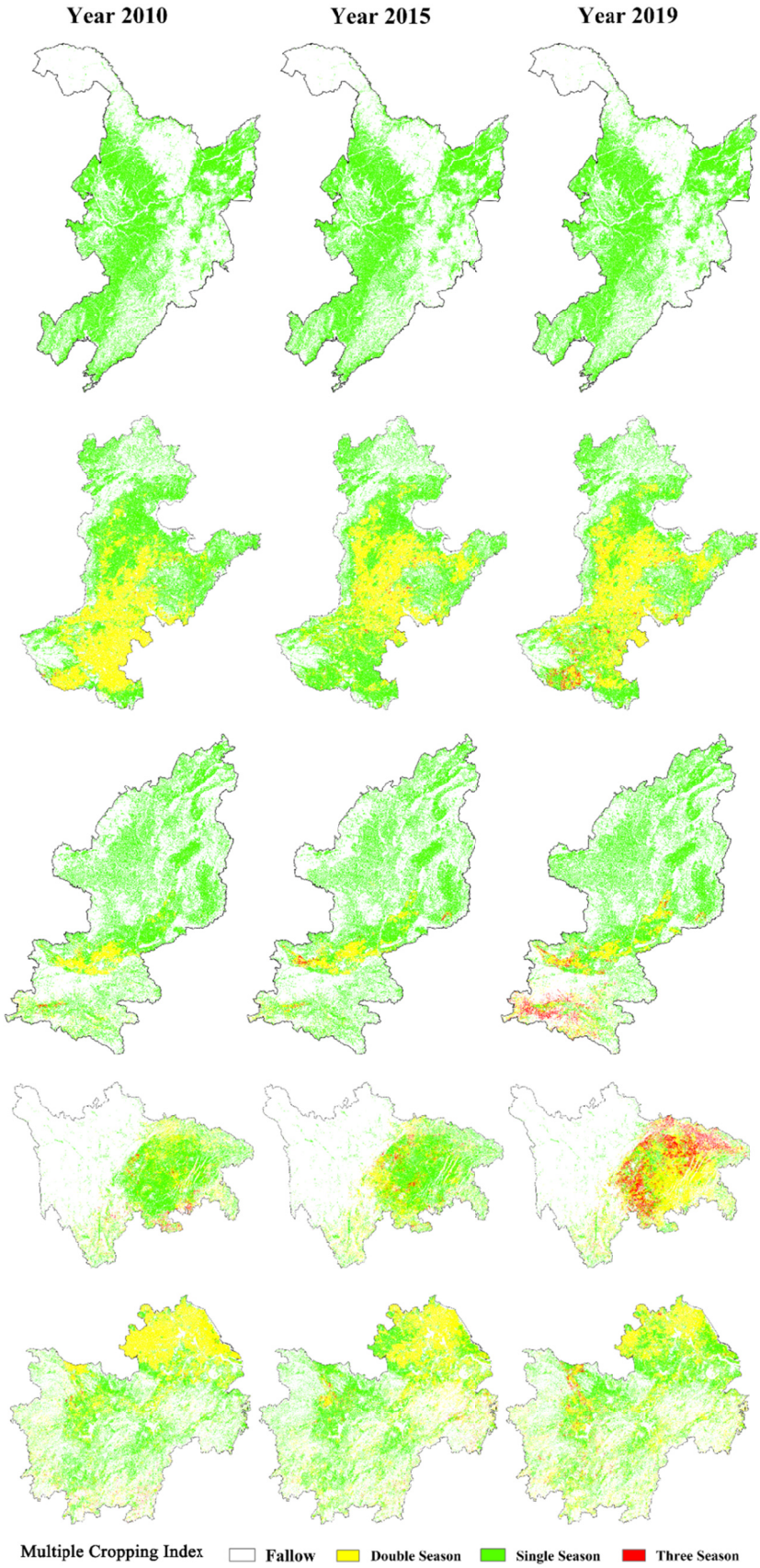

Figure 9. Comparison of the spatial distribution of the multiple cropping index in Northeast China and Huang-Huai-Hai region and Southwest China and Loess Plateau region and Yangtze River from 2010 to 2015 in 2019

It can be seen from Figure 9 that in the Yangtze River Middle and Lower Reaches region, mixed single and double-season crop planting is dominant, but with more single-season crops, resulting in an average replanting index range of 1.2-1.3, significantly higher than the other regions. In addition, the spatial distribution of the replanting index in this region shows a pattern of decreasing radiation from the center to the surrounding areas. As shown in Figure 8, it can be seen that the replanting index of arable land in this region has been on an overall downward trend from 2011 to 2019. There was a conversion from double-season crop planting to single-season crop planting, mainly concentrated in Anhui and Jiangsu provinces. The rapid economic development in these areas and the increasing non-agricultural employment opportunities have led to farmers investing less time in agricultural production to increase their income, thereby promoting the transformation of arable land from double-season crop planting to single-season crop planting.

4. Conclusions

Based on MODIS NDVI data and land use data, this paper used the second-order differencing method to obtain the spatial distribution of China's arable land replanting index from 2011 to 2019 and analyzed the spatiotemporal evolution characteristics of the replanting index during this period. The following main conclusions were drawn:

(1) There are significant differences in the spatial distribution of China's arable land replanting index. The Huang-Huai-Hai region is mainly cultivated with double-season crops, the Northeast Plain and Loess Plateau regions are mainly cultivated with single-season crops, and the Yangtze River South region is mainly cultivated with multiple-season crops. Overall, the replanting index in the northwest region is relatively low, while the replanting index in eastern provinces is relatively high, and the replanting index in southern regions is significantly higher than that in northern regions. Grain production is mainly based on single-season crops, with few three-season crops, most of which are distributed in southern regions.

(2) The overall trend of China's arable land replanting index during the study period was stable with a slight increase, but there were significant differences in specific situations across different regions. The replanting index in the Northeast Plain and Loess Plateau regions continued to increase, while the replanting index in the southern part of the Huang-Huai-Hai region and the Yangtze River Middle and Lower Reaches region showed a downward trend. Changes in the planting mode of arable land have led to significant changes in the replanting index of arable land.

Based on the research results mentioned above, to further improve the potential of arable land replanting, measures can be taken, such as stabilizing the planting area of double-season rice in the Yangtze River Middle and Lower Reaches region and curbing the reduction of double-season crop planting areas in this region, to promote grain production. On the other hand, the Huang-Huai-Hai region is the main grain-producing area in China, and reasonable ways should be adopted to promote the growth of the replanting index in this region. The use of remote sensing technology to obtain the replanting index of arable land has the advantages of convenience and efficiency, and it is believed that shortly soon, it will further develop and provide a scientific basis for improving land productivity and ensuring food security by promoting grain production.

References

Belgiu, M., & Csillik, O. (2018). Sentinel-2 cropland mapping using pixel-based and object-based time-weighted dynamic time warping analysis. *Remote Sensing of Environment, 204*, 509-523. https://doi.org/10.1016/j.rse.2017.10.005

Berger, K., Atzberger, C., Danner, M., D'Urso, G., Mauser, W., Vuolo, F., & Hank, T. (2018). Evaluation of the PROSAIL model capabilities for future hyperspectral model environments: A review study. *Remote Sensing, 10*(1), 85. https://doi.org/10.3390/rs10010085

Butt, A., Shabbir, R., Ahmad, S. S., & Aziz, N. (2015). Land use change mapping and analysis using Remote Sensing and GIS: A case study of Simly watershed, Islamabad, Pakistan. *The Egyptian Journal of Remote Sensing and Space Science, 18*(2), 251-259. https://doi.org/10.1016/j.ejrs.2015.07.003

Cian, F., Marconcini, M., & Ceccato, P. (2018). Normalized Difference Flood Index for rapid flood mapping: Taking advantage of EO big data. *Remote Sensing of Environment, 209*, 712-730. https://doi.org/10.1016/j.rse.2018.03.006

Estel, S., Kuemmerle, T., Levers, C., Baumann, M., & Hostert, P. (2016). Mapping cropland use intensity across Europe using MODIS NDVI time series. *Environmental Research Letters, 11*(2), 024015. https://doi.org/10.1088/1748-9326/11/2/024015

Feyisa, G. L., Palao, L. K., Nelson, A., Gumma, M. K., Paliwal, A., Win, K. T., ... Johnson, D. E. (2020). Characterizing and mapping cropping patterns in a complex agro-ecosystem: An iterative participatory mapping procedure using machine learning algorithms and MODIS vegetation indices. *Computers and Electronics in Agriculture, 175*, 105595. https://doi.org/10.1016/j.compag.2020.105595

Foley, J. A., DeFries, R., Asner, G. P., Barford, C., Bonan, G., Carpenter, S. R., ... Snyder, P. K. (2005). Global consequences of land use. *Science, 309*(5734), 570-574. https://doi.org/10.1126/science.1111772

Foley, J. A., Ramankutty, N., Brauman, K. A., Cassidy, E. S., Gerber, J. S., Johnston, M., ... Zaks, D. P. (2011). Solutions for a cultivated planet. *Nature, 478*(7369), 337-342. https://doi.org/10.1038/nature10452

Friedl, M. A., McIver, D. K., Hodges, J. C., Zhang, X. Y., Muchoney, D., Strahler, A. H., ... Schaaf, C. (2002). Global land cover mapping from MODIS: Algorithms and early results. *Remote Sensing of Environment, 83*(1-2), 287-302. https://doi.org/10.1016/S0034-4257(02)00078-0

Godfray, H. C. J., Beddington, J. R., Crute, I. R., Haddad, L., Lawrence, D., Muir, J. F., ... Toulmin, C. (2010). Food security: the challenge of feeding 9 billion people. *Science, 327*(5967), 812-818. https://doi.org/10.1126/science.1185383

Ibrahim, E. S., Rufin, P., Nill, L., Kamali, B., Nendel, C., & Hostert, P. (2021). Mapping crop types and cropping systems in Nigeria with sentinel-2 imagery. *Remote Sensing, 13*(17), 3523. https://doi.org/10.3390/rs13173523

Jiang, Y., Lu, Z., Li, S., Lei, Y., Chu, Q., Yin, X., & Chen, F. (2020). Large-scale and high-resolution crop mapping in China using sentinel-2 satellite imagery. *Agriculture, 10*(10), 433. https://doi.org/10.3390/agriculture10100433

Kuenzer, C., & Knauer, K. (2013). Remote sensing of rice crop areas. *International Journal of Remote Sensing, 34*(6), 2101-2139. https://doi.org/10.1080/01431161.2012.738946

Liu, E. K., He, W. Q., & Yan, C. R. (2014). 'White revolution' to 'white pollution'—Agricultural plastic film mulch in China. *Environmental Research Letters, 9*(9), 091001. https://doi.org/10.1088/1748-9326/9/9/091001

Marshall, M., & Thenkabail, P. (2015). Developing in situ non-destructive estimates of crop biomass to address issues of scale in remote sensing. *Remote Sensing, 7*(1), 808-835. https://doi.org/10.3390/rs70100808

Mishra, P., Pandey, C. M., Singh, U., Gupta, A., Sahu, C., & Keshri, A. (2019). Descriptive statistics and normality tests for statistical data. *Annals of Cardiac Anaesthesia, 22*(1), 67-72. https://doi.org/10.4103/aca.ACA_157_18

Ramoelo, A., Cho, M. A., Mathieu, R., Madonsela, S., Van De Kerchove, R., Kaszta, Z., & Wolff, E. (2015). Monitoring grass nutrients and biomass as indicators of rangeland quality and quantity using random forest modeling and WorldView-2 data. *International Journal of Applied Earth Observation and Geoinformation, 43*, 43-54. https://doi.org/10.1016/j.jag.2014.12.010

Ray, D. K., & Foley, J. A. (2013). Increasing global crop harvest frequency: recent trends and future directions. *Environmental Research Letters, 8*(4), 044041. https://doi.org/10.1088/1748-9326/8/4/044041

Ray, D. K., Ramankutty, N., Mueller, N. D., West, P. C., & Foley, J. A. (2012). Recent patterns of crop yield growth and stagnation. *Nature Communications, 3*(1), 1293. https://doi.org/10.1038/ncomms2296

Satyawan, M. Y., & Hooda, R. S. (2014). Cropping system analysis using geospatial approach: A case study of Sirsa District in Haryana, India. *International Journal of Science and Research, 3*(9), 2161-2167.

Veloso, A., Mermoz, S., Bouvet, A., Le Toan, T., Planells, M., Dejoux, J. F., & Ceschia, E. (2017). Understanding the temporal behavior of crops using Sentinel-1 and Sentinel-2-like data for agricultural applications. *Remote Sensing of Environment, 199*, 415-426. https://doi.org/10.1016/j.rse.2017.07.015

Xie, H., & Liu, G. (2015). Spatiotemporal differences and influencing factors of multiple cropping index in China during 1998-2012. *Journal of Geographical Sciences, 25*, 1283-1297. https://doi.org/10.1007/s11442-015-1234-3

Yan, H., Xiao, X., Huang, H., Liu, J., Chen, J., & Bai, X. (2014). Multiple cropping intensity in China derived from agro-meteorological observations and MODIS data. *Chinese Geographical Science, 24*, 205-219. https://doi.org/10.1007/s11769-013-0637-2

Yan, Y., Mao, Y., & Li, B. (2018). Second: Sparsely embedded convolutional detection. *Sensors, 18*(10), 3337. https://doi.org/10.3390/s18103337

Yang, N., Liu, D., Feng, Q., Xiong, Q., Zhang, L., Ren, T., ... Huang, J. (2019). Large-scale crop mapping based on machine learning and parallel computation with grids. *Remote Sensing, 11*(12), 1500. https://doi.org/10.3390/rs11121500

Acknowledgments

We greatly appreciate the undergraduate student Zhiying Chen for collecting a portion of the experimental data for this article.

Authors contributions

YHY proposed the study idea and designed the study. YHY and YHZ conducted all experiments and prepared the original manuscript. HYH provided a lot of very good suggestions for the analysis section of the paper. All the authors contributed to the manuscript revision.

Funding

This work was supported by the National Natural Science Foundation of China (grant number 42101361), and the scientific research project of higher education institutions in Anhui province.

Competing interests

The authors declare that they have no known competing financial interests or personal relationships that could have appeared to influence the work reported in this paper.

Informed consent

Obtained.

Ethics approval

The Publication Ethics Committee of the Canadian Center of Science and Education.

The journal's policies adhere to the Core Practices established by the Committee on Publication Ethics (COPE).

Provenance and peer review

Not commissioned; externally double-blind peer reviewed.

Data availability statement

The data that support the findings of this study are available on request from the corresponding author. The data are not publicly available due to privacy or ethical restrictions.

Data sharing statement

No additional data are available.